Plant Biology

H1 restricts euchromatin-associated methylation pathways from heterochromatic encroachment

Reviewed Preprint

Revised by authors after peer review.

About eLife's process

Reviewed preprint version 2
May 15, 2024 (this version)

Reviewed preprint version 1
September 12, 2023

Sent for peer review
May 25, 2023

Posted to preprint server
May 11, 2023

C. Jake Harris, **Zhenhui Zhong**, **Lucia Ichino**, **Suhua Feng**, **Steven E. Jacobsen**

Department of Molecular, Cell and Developmental Biology, University of California, Los Angeles, CA, USA • Department of Plant Sciences, University of Cambridge, Cambridge CB2 3EA, UK • Ministry of Education Key Laboratory for Bio-Resource and Eco-Environment, College of Life Sciences, Sichuan University, Chengdu 610065, China • Eli & Edythe Broad Center of Regenerative Medicine & Stem Cell Research, University of California, Los Angeles, Los Angeles, CA, USA • Howard Hughes Medical Institute, University of California, Los Angeles, CA, USA

Abstract

Silencing pathways prevent transposable element (TE) proliferation and help to maintain genome integrity through cell division. Silenced genomic regions can be classified as either euchromatic or heterochromatic, and are targeted by genetically separable epigenetic pathways. In plants, the RNA-directed DNA methylation (RdDM) pathway targets mostly euchromatic regions, while CMT DNA methyltransferases are mainly associated with heterochromatin. However, many epigenetic features - including DNA methylation patterning - are largely indistinguishable between these regions, so how the functional separation is maintained is unclear. The linker histone H1 is preferentially localized to heterochromatin and has been proposed to restrict RdDM from encroachment. To test this hypothesis, we followed RdDM genomic localization in an *h1* mutant by performing ChIP-seq on the largest subunit, NRPE1, of the central RdDM polymerase, Pol V. Loss of H1 resulted in NRPE1 enrichment predominantly in heterochromatic TEs. Increased NRPE1 binding was associated with increased chromatin accessibility in *h1*, suggesting that H1 restricts NRPE1 occupancy by compacting chromatin. However, RdDM occupancy did not impact H1 localization, demonstrating that H1 hierarchically restricts RdDM positioning. H1 mutants experience major symmetric (CG and CHG) DNA methylation gains, and by generating an *h1/nrpe1* double mutant, we demonstrate these gains are largely independent of RdDM. However, loss of NRPE1 occupancy from a subset of euchromatic regions in *h1* corresponded to loss of methylation in all sequence contexts, while at ectopically bound heterochromatic loci, NRPE1 deposition correlated with increased methylation specifically in the CHH context. Additionally, we found that H1 similarly restricts the occupancy of the methylation reader, SUVH1, and polycomb-mediated H3K27me3. Together, the results support a model whereby H1 helps maintain the exclusivity of heterochromatin by preventing encroachment from other competing pathways.

eLife assessment

This **important** study indicates a role for linker Histone H1 in protecting heterochromatic regions from certain types of repression. The experiments and data analysis that support the model for the role of linker Histone H1are **solid**, although additional experiments could provide a deeper mechanistic understanding. The study will be of broad interest to those interested in the role of chromatin in eukaryotic gene expression.

Introduction

Eukaryotic genomes are compartmentalized into euchromatic and heterochromatin regions (Ruiz-Velasco and Zaugg, 2017). In euchromatin, nucleosomes are more accessible, while in heterochromatin nucleosomes are more compacted and restrictive to transcription. Protein coding genes are typically euchromatic, while non-coding and repetitive elements more often reside in heterochromatin. However, transposable elements, which are targeted for DNA methylation and silencing, are found in both euchromatic and heterochromatic regions of the genome (Bourque et al., 2018). The pathways responsible for deposition of methylation and silencing of TEs in these different regions are functionally and genetically distinct (Du et al., 2015).

In plants, euchromatic repetitive regions are targeted by the RNA-directed DNA methylation pathway (RdDM) (Erdmann and Picard, 2020), in which the concerted action of non-coding RNA polymerases and small RNAs direct the DNA methyltransferase, DRM2, to specific sites of the genome. Newly invading genetic elements are targeted by the 'non-canonical' RdDM pathway, and involve the action of Pol II derived small RNAs (Cuerda-Gil and Slotkin, 2016). Once established, the canonical RdDM pathway takes over, whereby small RNAs are generated by the plant-specific polymerase IV (Pol IV). In both cases, a second plant-specific polymerase, Pol V, is an essential downstream component. Pol V transcribes scaffold transcripts to which Argonaute bound small RNAs can bind through base complementarity to recruit DRM2 to direct DNA methylation (Wierzbicki et al., 2009, 2008; Zhong et al., 2014). The recruitment of Pol V to chromatin is stabilized by interaction with the DNA methylation readers SUVH2 and SUVH9 (Johnson et al., 2014). However, methylation alone is not sufficient to explain Pol V occupancy, as Pol V is restricted to the edges of long TEs and euchromatic methylated regions, despite methylation levels being high in the bodies of long TEs and in heterochromatin (Zhong et al., 2012). Therefore, additional mechanisms must exist to regulate Pol V occupancy.

Heterochromatin is targeted for DNA methylation and silencing by CMT methyltransferases (Stroud et al., 2014; Zemach et al., 2013). CMT3 and CMT2 are responsible for CHG and CHH methylation maintenance, respectively, at these regions. The CMTs form an epigenetic feedback loop with the KYP family of H3K9me2 methyltransferases, thereby maintaining high levels of repression-associated non-CG methylation and H3K9me2 at heterochromatic regions of the genome (Du et al., 2014, 2012; Li et al., 2018). As both DNA methylation and H3K9me2 are known to recruit components of the RdDM pathway (Johnson et al., 2014; Law et al., 2013), it is unclear how these regions remain functionally separated from RdDM.

The linker histone H1 associates with nucleosomes to modulate chromatin accessibility and higher order structures (Saha and Dalal, 2021). H1 binds to linker DNA as it exits from the nucleosome dyad and reduces linker DNA flexibility (Bednar et al., 2017). In plants, H1 is preferentially associated with heterochromatin, where it contributes to chromatin compaction (Bourguet et al., 2021; Choi et al., 2020; Rutowicz et al., 2019). Genetic evidence suggest that the chromatin

remodeler DDM1 displaces H1 at heterochromatic TEs to facilitate access of CMT methyltransferases (Zemach et al., 2013), while biochemical data suggests that this effect could be indirect, via DDM1s interaction with the heterochromatin associated histone variant, H2A.W (Osakabe et al., 2021). Why DDM1 grants CMTs but not RdDM access to H1-containing nucleosomes is not clear. Recent structural data shows that nucleosome bound DDM1 promotes DNA sliding (Liu et al., 2024), which may be sufficient for CMT to deposit methylation, but not for the RdDM machinery to become established. H1 also plays a key role in shaping nuclear architecture and preventing ectopic polycomb-mediated H3K27me3 deposition in telomeres (Teano et al., 2023).

Since H1 physically locks genomic DNA to the nucleosome and is preferentially associated with heterochromatin, it is a promising candidate for preventing RdDM encroachment into these regions. Recent evidence supports this hypothesis, with RdDM associated small RNAs becoming more heterochromatically enriched in *h1* knockouts (Choi et al., 2021; Papareddy et al., 2020). However, small RNAs are not a direct readout of functional RdDM activity and Pol IV dependent small RNAs are abundant in regions of the genome that do not require RdDM for methylation maintenance and that do not contain Pol V (Stroud et al., 2014). Here we directly tested whether RdDM occupancy is affected by loss of H1, by taking advantage of an endogenous Pol V antibody (which recognizes Pol V's largest subunit, NRPE1). We found that *h1* antagonizes NRPE1 occupancy throughout the genome, particularly at heterochromatic regions. This effect was not limited to RdDM, similarly impacting both the methylation reader complex component, SUVH1 (Harris et al., 2018) and polycomb-mediated H3K27me3 (Teano et al., 2023). These results suggest that H1 acts in part to restrict the function of other epigenetic pathways.

Results

To understand how H1 affects RdDM occupancy, we performed chromatin immunoprecipitation followed by sequencing (ChIP-seq) with a native antibody against NRPE1 (the largest catalytic subunit of Pol V, previously validated (Liu et al., 2018)). Two biological replicates of ChIP-seq in wild type control Col-0 and in *h1.1-1/h1.2-1* double mutant (hereafter referred to as WT and *h1*, respectively) were performed. As previously reported (Bohmdorfer et al., 2016; Liu et al., 2018; Zhong et al., 2012), NRPE1 was enriched over short TEs and at the edges of long TEs in WT (**Fig. 1A-B**). In the *h1* mutant, however, NRPE1 enrichment was markedly increased, with NRPE1 invading the heterochromatic bodies of long TEs (**Fig. 1A-B**). The negative correlation between NRPE1 enrichment and TE length observed in WT was reverted in the *h1* mutant (**Fig. 1C**). This suggests that mutation of *h1* facilitates the invasion of NRPE1 to more heterochromatic regions, in which long TEs tend to reside (Bourguet et al., 2021; Zemach et al., 2013). Consistent with this, NRPE1 increased more over heterochromatin associated CMT2 dependent hypo-CHH differentially methylated regions (DMRs) than at the RdDM associated DRM2 dependent CHH sites (**Fig. 1D**). The preferential enrichment of NRPE1 in *h1* was more pronounced at TEs that overlapped with heterochromatin associated mark, H3K9me2 (**Fig. 1E**). Comparing NRPE1 occupancy over TEs that had previously been classified by as either 'euchromatic' or 'heterochromatic' (based on a broad range of features and small RNA expression dynamics during embryonic development (Papareddy et al., 2020), again, we found a striking increase in NRPE1 at heterochromatic over euchromatic TEs in *h1* (**Fig. 1F**). From a chromosomal viewpoint, NRPE1 was preferentially enriched over pericentromeric regions in *h1*, and showed corresponding depletion from the more euchromatic chromosomal arms (**Fig. 1G**, Supplementary Fig. 1). Importantly, we found no evidence for increased expression of NRPE1 or other methylation pathway components known to be involved in Pol V loading or stability in the *h1* mutant (Supplementary Table 1). Together, the results indicate that H1 broadly restricts NRPE1 access to chromatin, and that this effect is more pronounced in heterochromatic regions of the genome. As H1 itself is preferentially localized to heterochromatin (see **Fig. 1B,D**,F) (Bourguet et al., 2021; Choi et al., 2020), this suggests that H1 directly antagonises RdDM occupancy.

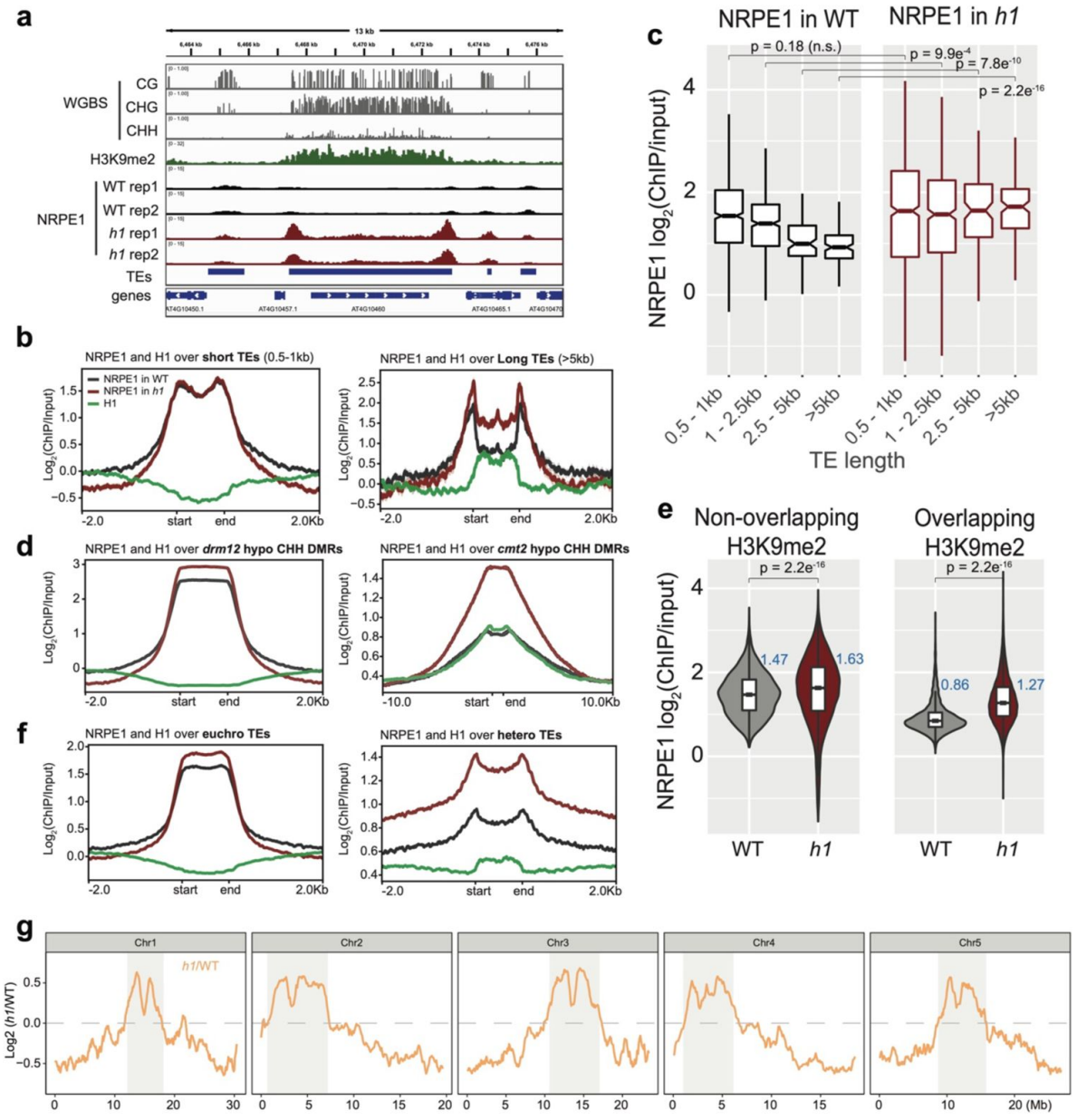

Figure 1

NRPE1 accumulates in heterochromatin in an *h1* mutant background:

A) Genome browser image showing increased NRPE1 enrichment in *h1* over heterochromatic (long, H3K9me2 enriched) and not euchromatic (short, not H3K9me2 enriched) TEs. B) metaplot showing ChIP-seq enrichment of NRPE1 in WT vs. *h1*, and H1 occupancy in WT for reference (data from GSE122394), at short vs. long TEs. C) boxplot showing association between NRPE1 and TE length in WT and *h1*. wilcoxon rank sum test p-values indicated. D) As in B) for *drm12* vs. *cmt2* hypo CHH DMRs. E) Violin plot inlaid with boxplot showing enrichment of NRPE1 at TEs that overlap with H3K9me2 peaks, vs. TEs that do not, in WT vs. *h1*. Boxplot medians are shown in blue. Wilcoxon rank sum test p-values indicated. F) as in B) at euchromatic vs. heterochromatic TEs. G) Chromosomal plots showing NRPE1 enrichment in *h1* as compared to WT, with pericentromeric regions denoted in grey.

One mechanism by which H1 could restrict RdDM access is by promoting chromatin compaction. Consistent with this idea and previous reports (Bourguet et al., 2021; Choi et al., 2020; He et al., 2019; Rutowicz et al., 2019), we observed increased accessibility in heterochromatic regions in *h1*, which mirrored the preferential recruitment of NRPE1 to heterochromatin (Supplementary Fig. 2AB). Loss of H1 mediated compaction in heterochromatin may be the indirect result of loss of heterochromatin associated marks such as H3K9me2. To examine this possibility, we performed H3K9me2 ChIP-seq, and although we observed some minor reductions in H3K9me2 in *h1*, the losses were not preferentially in heterochromatin where we see the majority of NRPE1 gain (Supplementary Fig. 2CD). While we cannot exclude the possibility that other heterochromatin associated marks are altered, the data suggests that H1 primarily affects the accessibility, rather than the nature of chromatin at these heterochromatic regions.

To determine whether the antagonistic relationship between H1 and NRPE1 is reciprocal, we performed ChIP-seq using an endogenous antibody for H1, with two biological replicates in the WT and *nrpe1* mutant backgrounds. H1 levels were broadly unchanged in *nrpe1* at TE regions (**Fig. 2A**). Similarly, over NRPE1 defined peaks (where NRPE1 occupancy is strongest in WT) we observed no change in H1 occupancy in *nrpe1* (**Fig. 2B**). The results indicate that H1 does not invade RdDM regions in the *nrpe1* mutant background.

Next, we asked whether ectopic recruitment of RdDM may be sufficient to evict H1 from the genome. For this, we took advantage of the ZF-DMS3 transgenic lines that we previously characterized, in which zinc finger (ZF) fused DMS3 can recruit endogenous NRPE1 to >10,000 ectopic sites throughout the genome, corresponding to ZF 'off-target' binding sites (Gallego-bartolome et al., 2019). With these lines, we performed NRPE1 and H1 ChIP-seq in parallel. Compared to the non-transgenic control, we confirmed that NRPE1 was highly enriched at these 'off-target' regions (**Fig 2C**). However, with the same material, we observed no depletion of H1 at the ectopically bound NRPE1 sites (**Fig. 2C**). We validated the quality of our H1 ChIPs, demonstrating antibody specificity, showing that they follow the previously described profiling patterns over H2A.W associated TEs (Bourguet et al., 2021), H3K27me3 marked/unmarked genes (Teano et al., 2023), and that H1.2 occupancy (Teano et al., 2023) is similarly enriched over our H1 peaks (Supplementary Fig. 3). To exclude the possibility that NRPE1 alone may be insufficient to evict H1, but that the fully functioning RdDM pathway may be required (which constitutes at least 32 described proteins acting in concert (Matzke and Mosher, 2014)), we focused on the subset of ZF-DMS3 off-target sites that experience hyper-CHH methylation (Gallego-bartolome et al., 2019). The gain of ectopic methylation at these regions indicates that the full RdDM pathway is recruited and functions to deposit *de novo* methylation. However, even at these regions where H1 is mildly enriched in WT, we saw no evidence for H1 depletion in the ZF-DMS3 transgenic lines (**Fig. 2D**). Together, these results indicate that H1 hierarchically and non-reciprocally restricts RdDM from overaccumulation in heterochromatin.

Given our observation that NRPE1 is redistributed in *h1*, we wondered whether this could help to explain some of the unusual methylation defects observed in the *h1* mutant. For instance, *h1* mutants experience contrasting loss and gain of DNA methylation at euchromatic and heterochromatic TEs, respectively (Bourguet et al., 2021; Zemach et al., 2013). Previous explanations to account for this suggested that the *h1* afforded increased accessibility of euchromatic TEs may promote increased access by activation-associated chromatin modifying enzymes, which in turn antagonise DNA methylation (Zemach et al., 2013). Another non-mutually exclusive scenario is that euchromatic loss and heterochromatic gain of methylation is caused by the relative shift of RdDM from euchromatin to heterochromatin. To directly test this possibility, we generated two independent NRPE1 CRISPR knockouts in the *h1* mutant background (Supplementary Fig. 4AB), and performed whole genome bisulfite sequencing (WGBS) analysis, alongside *nrpe1*, *h1* and WT controls. We confirmed *nrpe1* loss of function in the independent CRISPR KO lines by plotting CHH methylation over NRPE1 associated high confidence DMRs (Zhang et al., 2018), finding that CHH methylation is entirely abolished over these regions in

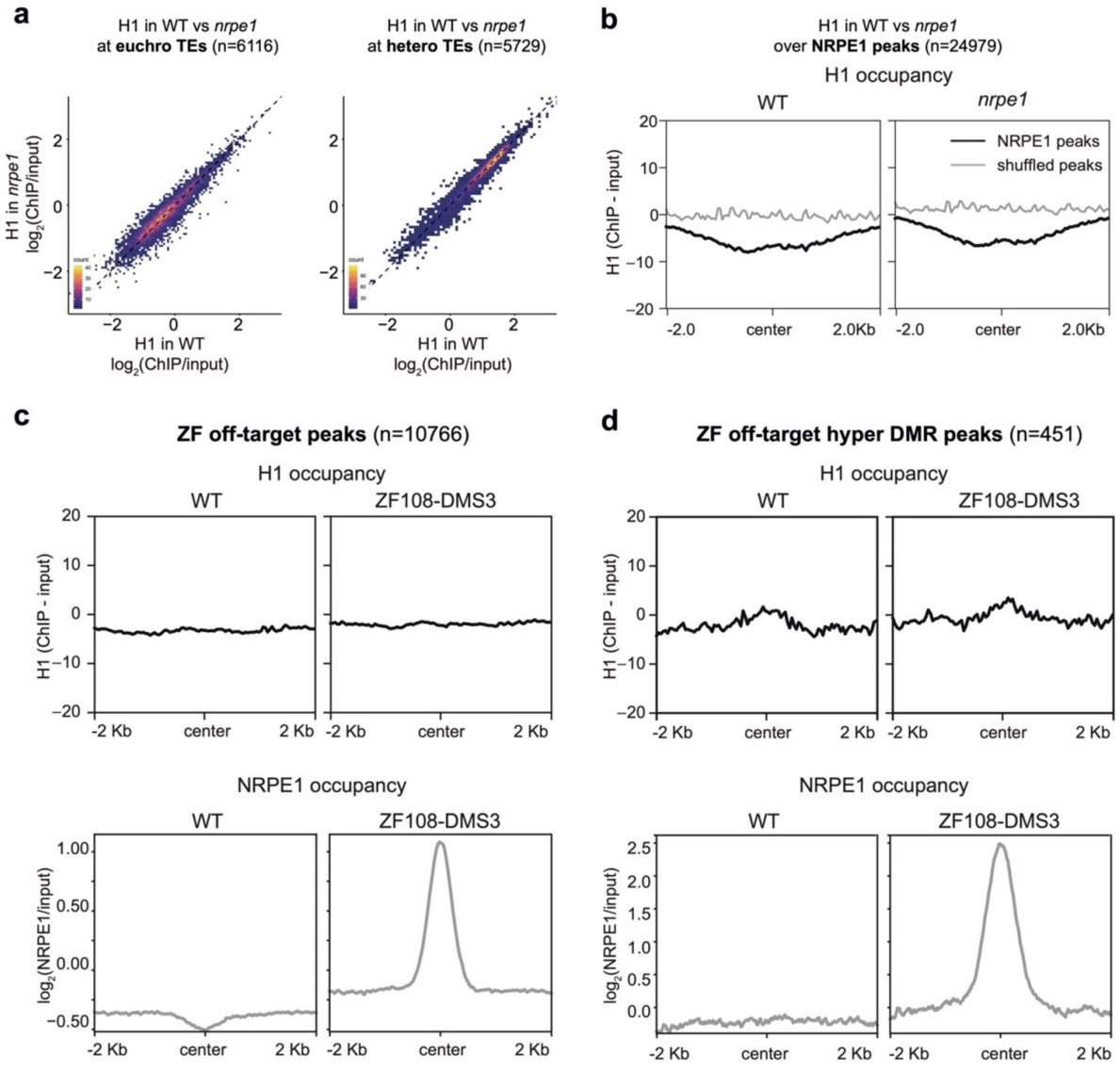

Figure 2

RdDM does not reciprocally affect H1 localization:

A) Scatter plot showing H1 enrichment in WT vs. *nrpe1* at euchromatic vs heterochromatic TEs. B) Metaplot showing H1 enrichment at NRPE1 peaks in WT vs. *nrpe1* C) H1 and NRPE1 occupancy at ZF-DMS3 off target peaks. Upper panel: H1 occupancy in WT vs. ZF108-DMS3. Lower panel: NRPE1 occupancy in WT vs. ZF108-DMS3. Chromatin from the same sample was used for both H1 and NRPE1 ChIP-seq data, so the lower panel serves as a control showing that ZF108-DMS3 is recruited to these off-target regions in these samples, despite H1 localisation remaining unchanged. D) Same as C) at the subset of regions where CHH methylation is gained in ZF108-DMS3 (Liu et al 2018), indicating that the fully functioning RdDM pathway is recruited to these regions.

both *nrpe1/h1* lines (Supplementary Fig. 4C). By analysis of chromosome level DNA methylation patterns in the different mutant backgrounds, we found that the striking pericentromeric increase in CG and CHG methylation observed in *h1*, is almost entirely independent of RdDM, as it was not rescued in *nrpe1/h1* (**Fig. 3A**, Supplementary Fig. 5). In contrast, CHH methylation was mostly unaltered between the genotypes at the chromosome scale, with evidence for a slight reduction of CHH in the *h1/nrpe1* double mutant as compared to *h1* alone (**Fig. 3A**, Supplementary Fig. 5).

Next, we compared methylation levels in euchromatic versus heterochromatic TEs. Heterochromatic TEs experienced major increases in CG and CHG methylation in *h1* as previously reported (Zemach et al., 2013), and these were independent of NRPE1 function, as the same increases were observed in *nrpe1/h1* (**Fig. 3B**). CHH levels were largely unchanged at heterochromatic TEs in all mutant backgrounds (**Fig. 3B**). At euchromatic TEs, CG and CHG methylation levels were largely unchanged in *h1*, while CHH levels were markedly reduced as previously reported (**Fig. 3C**). CHH methylation levels were further reduced in *nrpe1*, consistent with the well-established role of RdDM in maintaining CHH at euchromatic TEs (Stroud et al., 2013), with the additional mutation of *h1* in *nrpe1/h1* having a minimal effect (**Fig. 3C**). However, we noticed that the loss of CHG methylation in *nrpe1* was largely rescued in the *nrpe1/h1* double mutant (**Fig. 3C**). This striking effect was specific to euchromatic TEs. NRPE1 is therefore required for CHG methylation maintenance at euchromatic TEs and in the absence of H1, loss of RdDM can be functionally compensated for by other methylation pathways. This compensation is likely due to the action of CMT3 (Stroud et al., 2014; Zemach et al., 2013). The effect is reminiscent of *h1*'s amelioration of methylation loss in the chromatin remodeler mutant, *ddm1* (Zemach et al., 2013), and further supports a role for H1 in demarcating the boundary between heterochromatic and euchromatic methylation pathways.

Calling DMRs in the mutant backgrounds, we found that *h1* hyper CHG DMRs were by far the most numerous as compared to any other context (**Fig. 4A**). Consistent with the average methylation chromosomal and TE plots, these hyper CHG DMRs were highly enriched over pericentromeric heterochromatin (**Fig. 4B**). To gain insight into the functional context of methylation in these regions, we performed overlap analysis between *h1* hyper CHG DMRs and DMRs from 96 other Arabidopsis gene silencing mutants that were published previously (Stroud et al., 2013). Building similarity matrices based on pairwise overlapping scores (Co-Occurrence Statistics), we observed separation of clustering of mutants belonging to different functional pathways (**Fig. 4C**, Supplementary Fig. 6), consistent with previous studies (Stroud et al., 2013; Zhang et al., 2018). The *h1* hyper CHG DMRs clustered primarily with components of the CG maintenance pathway, including *met1* and *vim1/2/3* (**Fig. 4D**). Interestingly, the *h1* hyper CHG DMRs also clustered and correlated strongly with *ddm1* hyper CHH DMRs. As heterochromatic transposons are known to transition from a state of quiescence to being actively targeted by RdDM in the *ddm1* mutant (Panda et al., 2016), this again suggests that H1 controls regions of the genome that are susceptible to spurious RdDM targeting.

While the majority of methylation changes observed in *h1* (hyper CG and CHG) were entirely independent of NRPE1, in the chromosomal plots we noted a subtle depletion of CHH methylation in the *h1/nrpe1* double mutant as compared to *h1* alone (**Fig. 3A**), suggesting that redistribution of NRPE1 may have functional consequences on methylation patterning. To explicitly investigate these ectopically bound loci, we compared NRPE1 enrichment in WT versus *h1* and identified 15,075 peaks that have significantly higher NRPE1 signal in the *h1* mutant. At these regions, CG and CHG methylation changes broadly mirrored that of heterochromatic TEs, again supporting the notion that NRPE1 primarily redistributes to heterochromatic regions of the genome in *h1* (**Fig. 5A**, Supplementary Fig. 7A). However, we also observed a significant depletion of CHH methylation at these regions in the *nrpe1/h1* double mutant, as compared to either the *h1* and *nrpe1* alone, which was not observed when looking at heterochromatic TEs as a whole (compare **Fig. 5A** to **Fig. 3B**). This indicates that NRPE1 facilitates active deposition of CHH methylation at these newly bound locations. Reciprocally, we asked how methylation changes at regions of the

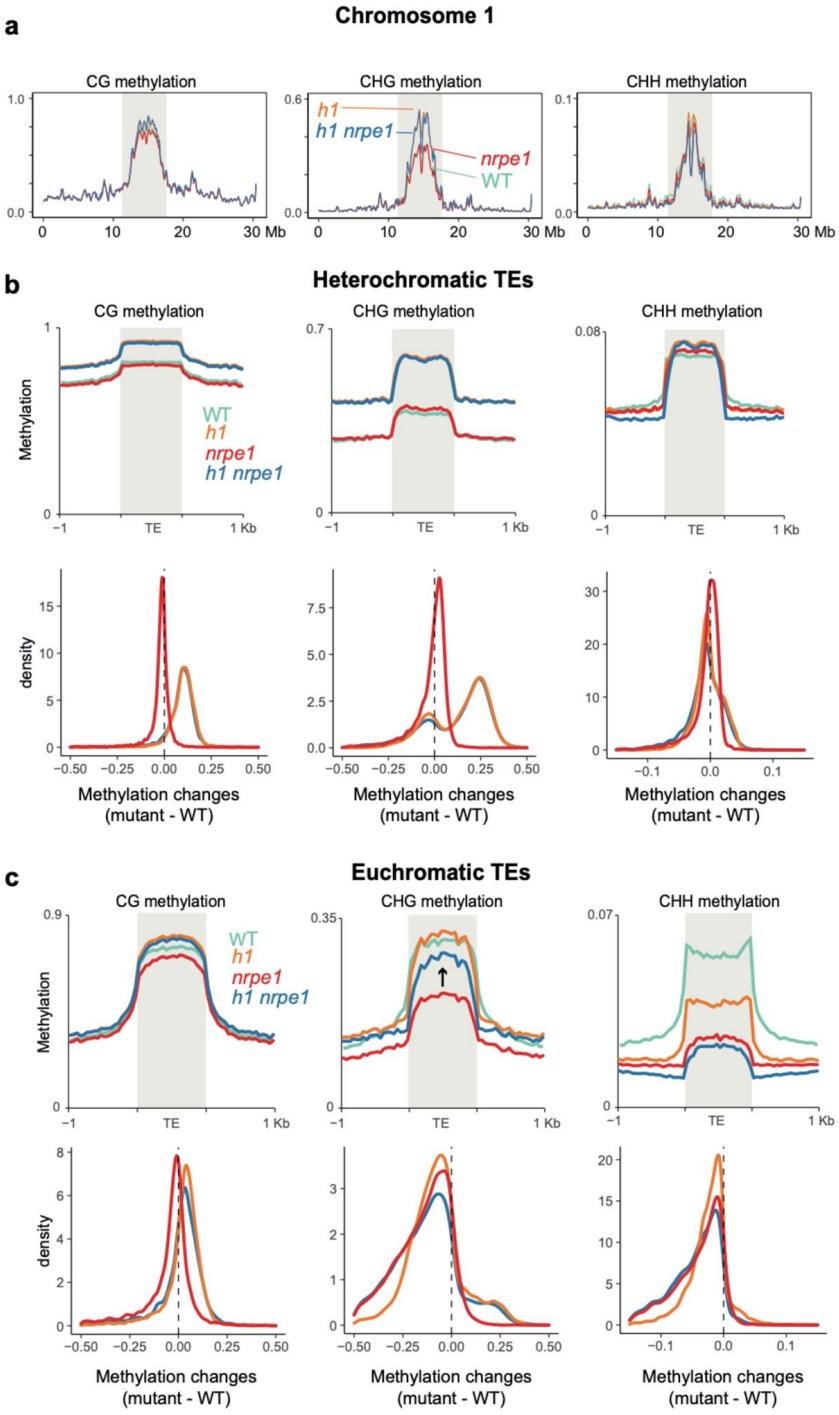

Figure 3

Major CG and CHG methylation gains in *h1* are independent of RdDM:

A) Chromosomal view of DNA methylation levels (average of 10kb windows) in the genotypes indicated on chromosome 1. Y-axis indicates fraction methylation (0-1). B) Methylation level over heterochromatic TEs. Upper panel: methylation metaplots, Lower panel - kernel density plots. In the kernel density plots, the average methylation is calculated for each TE in both mutant and WT, then then the methylation difference is calculated. The plot shows the frequency density of TEs that gain/lose DNA methylation in the regions in the mutants indicated. C) Methylation level over euchromatic TEs. Upper panel: metaplots, Lower panel - kernel density plots (as above). Arrow highlights the gain in CHG methylation in the *h1/nrpe1* double mutant, as compared to *nrpe1* alone.

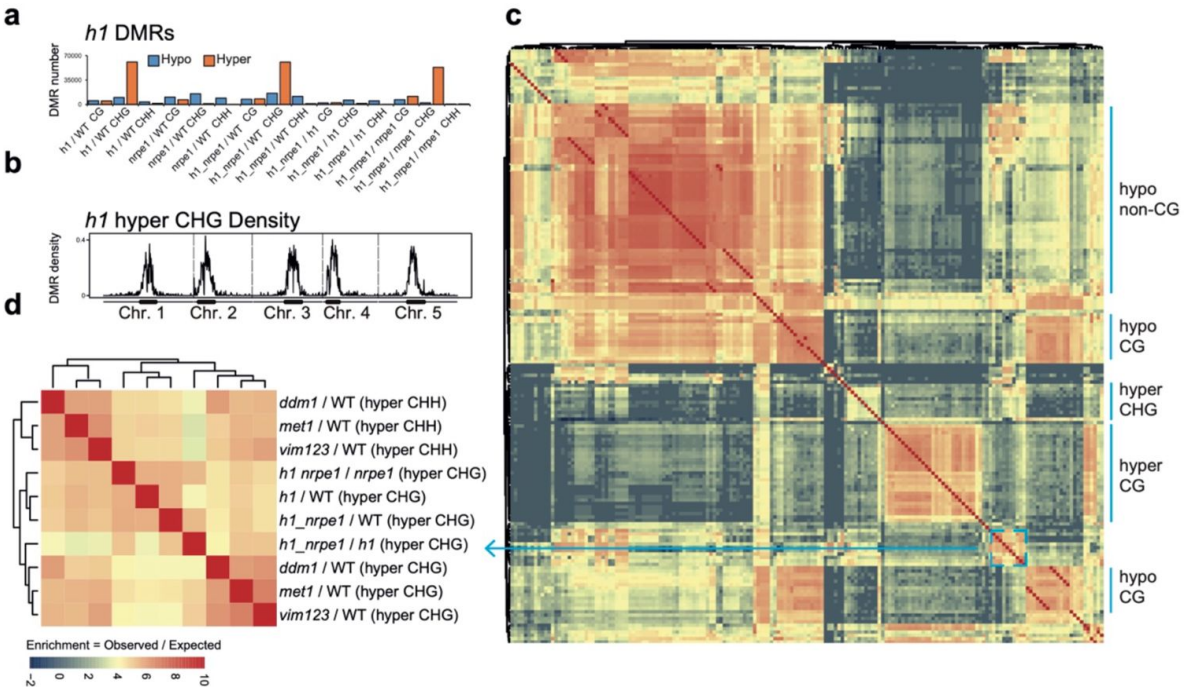

Figure 4

Overlap analysis of *h1* hyper CHG DMRs with 96 methylation mutants:

A) Number of hypo vs hyper DMRs in genotype comparisons indicated. B) *h1* hyper CHG DMR frequency density plot over Chromosomes 1-5. C) Similarity matrix based on pairwise overlapping scores (Co-Occurrence Statistics) of DMRs from 96 whole methylomes.. The labels on the right summarise the major functional categories of the methylation mutant genotypes in the cluster block. (individual genotypes are shown in Supplementary Figure 6). The colour scale represents the number of observed DMR overlaps between the pairwise comparison indicated over the number of overlaps expected by chance (DMRs randomly distributed throughout the genome). Red means highly enriched overlapping DMRs (similar genomic distribution), blue means highly non-overlapping (different genomic distribution) D) Zoomed in view of the cluster containing *h1* hyper CHG DMRs C) (see blue box and arrow).

genome that lose NRPE1 in *h1* (1,859 peaks), and we found that methylation levels are significantly depleted in all three contexts (CG, CHG and CHH) in the *h1*, *nrpe1* and *nrpe1/h1* double mutant backgrounds (**Fig. 5B**, Supplementary Fig. 7B and 8). The mirrored loss and gain of methylation with changes in NRPE1 occupancy indicates that NRPE1 redistribution in *h1* directly impacts methylation patterning *in cis*.

The results thus far support a model whereby H1 prevents RdDM encroachment into heterochromatin. As H1 likely restricts access by reducing chromatin accessibility at these regions, we reasoned that this effect would not be RdDM specific and could affect other machinery in a similar manner. The SUVH1 methyl binding protein directly binds CHH methylation *in vitro*, yet shows strong preferential recruitment to RdDM over CMT dependent sites *in vivo* (Harris et al., 2018). Along with SUVH3, SUVH1 functions to protect the expression of genes residing nearby to RdDM targeted transposable elements by recruiting DNAJ1/2 transcriptional activators. We therefore wondered whether the SUVH1's occupancy might also be affected by H1. To test this, we performed ChIP-seq on SUVH1-3xFLAG in an *h1* mutant background (**Fig. 6A**). As with NRPE1, SUVH1 was generally enriched throughout the genome in *h1*, but the effect was strongest over heterochromatin (long TEs, *cmt2*-dependent hypo-CHH DMRs, and heterochromatic TEs, **Fig. 6B**). At the transcript level, we saw no evidence that SUVH1 or related complex components are upregulated in the *h1* mutant background (Supplementary Table 1), however, we cannot rule out the possibility that the SUVH1-3xFLAG transgene is expressed more highly in *h1*. Teano et al recently showed that polycomb dependent H3K27me3 is redistributed in *h1*. We compared sites that gain NRPE1 to sites that gain H3K27me3 in *h1*, finding a statistically significant overlap (2.4 fold enrichment over expected, hypergeometric test p-value $2.1e^{-71}$). Reciprocally, sites that lose NRPE1 were significantly enriched for overlap with H3K27me3 loss regions (1.6 fold over expected, hypergeometric test p-value $1.4e^{-4}$). This indicates that RdDM and H3K27me3 patterning are similarly modulated by H1. To directly test this, we reanalysed the H3K27me3 ChIP-seq data from Teano et al., finding coincident enrichment and depletion of H3K27me3 at sites that gain and lose NRPE1 in *h1* (**Fig 6E**). Therefore, H1 acts in a non-RdDM specific manner, to prevent euchromatic machinery from heterochromatic encroachment, likely through promoting nucleosome compaction and restricting access to chromatin.

Discussion

Here we show that loss of H1 results in redistribution of RdDM from euchromatic to heterochromatic regions, consistent with recent findings from small RNA data (Choi et al., 2021; Papareddy et al., 2020). This ectopic accumulation results in modest but detectable NRPE1-dependent methylation, and it would be interesting to determine whether Pol V transcript production and DRM2 methyltransferase recruitment occurs in a similar manner to euchromatin in these regions. It is important to note that NRPE1 binding was generally increased in the *h1* mutant (both euchromatin and heterochromatin), consistent with H1's widespread occupancy through the genome, but that the effect was strongest in heterochromatin where H1 shows maximal enrichment (Bourguet et al., 2021; Choi et al., 2020; Rutowicz et al., 2019). The antagonism of RdDM by H1 is non-reciprocal, as H1 levels were not affected by RdDM loss, or artificial gain at ectopic regions of the genome. H1-mediated restriction could be in part due to its structural capacity to reduce linker DNA flexibility (Bednar et al., 2017), thereby reducing polymerase access to unwind and interact with genomic DNA. Pol V requires the DDR complex for efficient association with chromatin (Wongpalee et al., 2019), so the presence of H1 could present an additional barrier to this complex. Mammalian H1 has been shown to compact chromatin in part through the phase separating property of its highly charged intrinsically disordered domain (Gibson et al., 2019). Consistent with this, very recent work in Arabidopsis showed that H1 induced phase separation and that this capacity was essential for the stability of heterochromatic nuclear foci (He et al., 2024). Therefore, another possibility is that high H1 occupancy creates a biophysical environment that excludes Pol V and related complexes. Our data

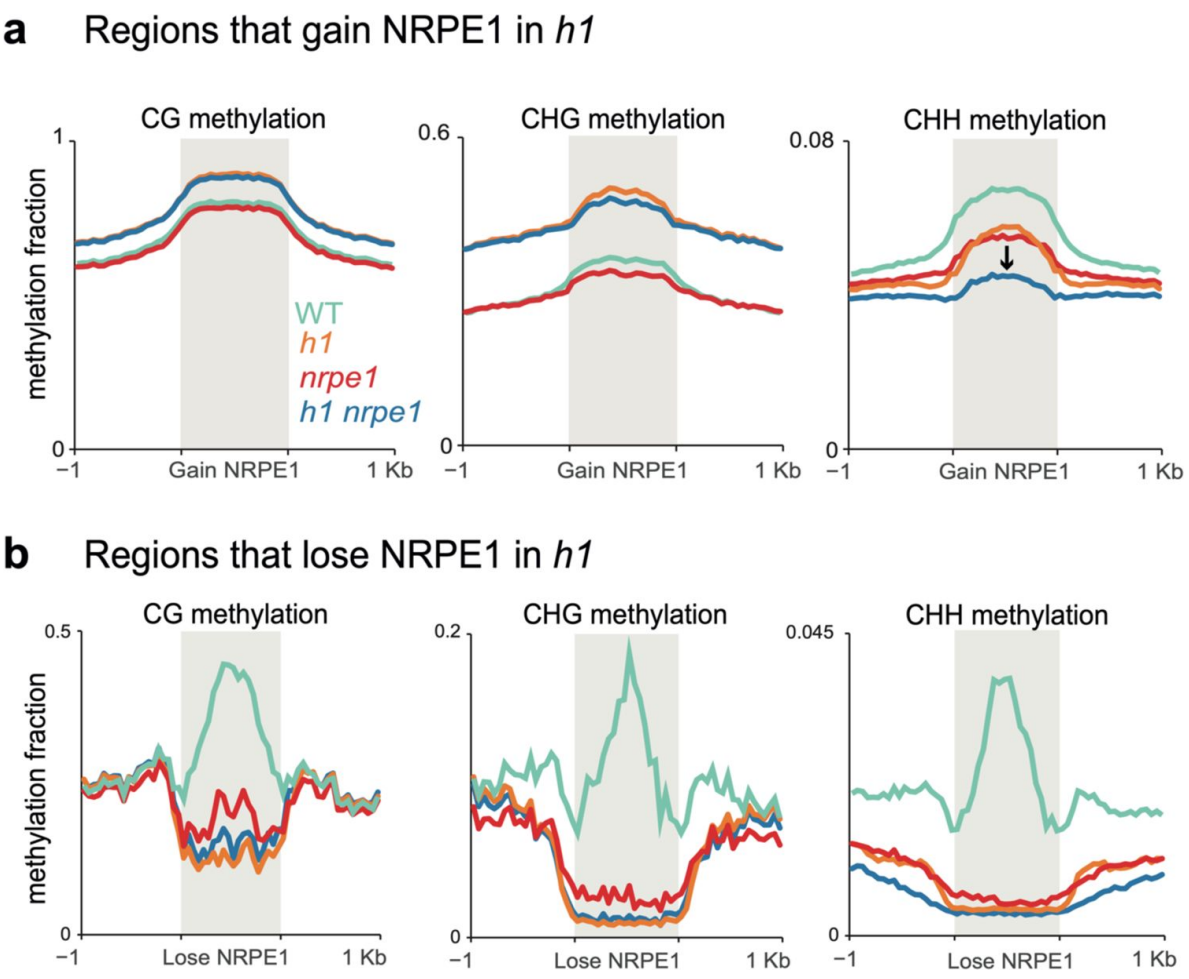

Figure 5

Patterns of NRPE1 re-localisation in *h1* show corresponding methylation changes: A) Methylation metaplot in the genotypes indicated over regions of the genome that gain NRPE1 in *h1*. Arrow highlights the change in average CHH methylation in the *h1/nrpe1* double mutant as compared to the single mutants. B) Methylation metaplot of the genotypes indicated over regions of the genome that lose NRPE1 in *h1*.

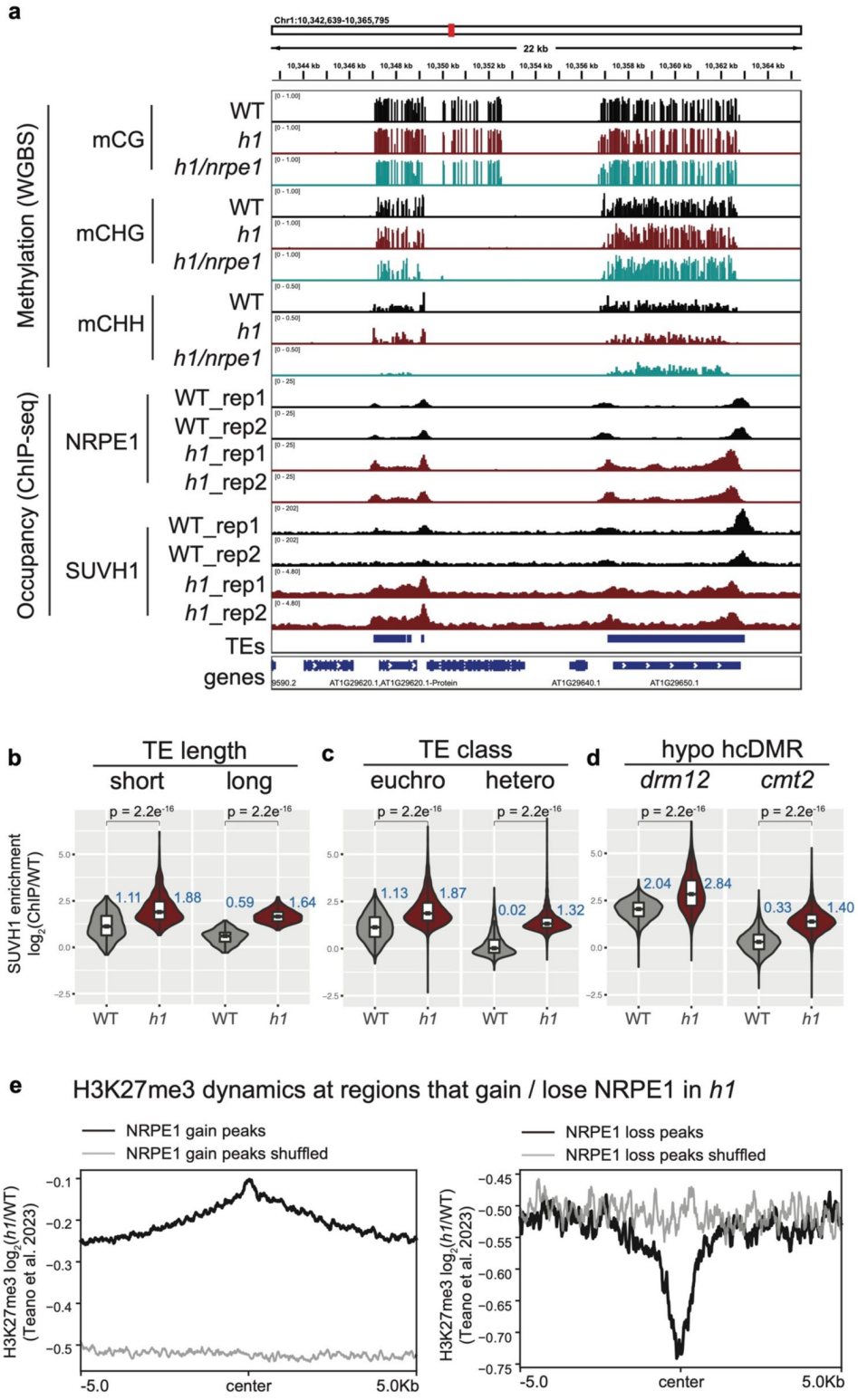

Figure 6

SUVH1 encroaches heterochromatin in an *h1* mutant background:

A) Genome browser image showing SUVH1 re-localisation in *h1* mirrors that of NRPE1. B-D) Boxplot inlaid violin plots showing SUVH1 enrichment in WT vs *h1* at short vs long TEs (B), at euchromatic vs heterochromatic TEs (C) and at drm12 vs cmt2 hypo CHH DMRs (D).

together with the observed heterochromatic encroachment of Pol IV dependent small RNAs in *h1* (Choi et al., 2021; Papareddy et al., 2020), along with H1's recently described role in preventing spurious antisense transcription at protein coding genes (Choi et al., 2020), support a polymerase indiscriminate model for H1's antagonism.

Small RNAs are relatively abundant in heterochromatin, despite Pol lV and RdDM being dispensable for methylation in these regions (Stroud et al., 2014). This suggests that Pol IV occupies heterochromatin, but that RdDM is either impotent for methylation deposition or acts redundantly with the CMT/KYP pathway. Here we detect NRPE1-dependent methylation at heterochromatic loci in *h1*, and combined with the finding that Pol V does not appreciably enter these regions in WT, suggests that H1 prevents RdDM from fully mobilizing in these regions by blocking Pol V. Recent evidence suggests that Pol V can be directly recruited by small RNAs to establish methylation (Sigman et al., 2021), and therefore mechanisms that preclude Pol V recruitment to heterochromatin would be particularly crucial in preventing redundant RdDM activity at regions where methylation has already been established.

In *Arabidopsis thaliana*, RdDM targets evolutionarily young transposable elements (Zhong et al., 2012). H1 therefore helps to improve the efficiency of RdDM by focusing it upon TEs with the greatest potential to mobilize. As transposons age, they eventually become targeted by CMTs. How this transition occurs is unclear, but our results indicate a potential role for progressive accumulation of H1 in this process. Interestingly in tomato, CMTs rather than RdDM target the evolutionarily younger elements (Wang and Baulcombe, 2020), therefore it will be important to determine whether H1 plays a similar role in maintaining the barrier between methylation pathways in this context. Recent work has shown that H1 co-operates with H2A.W to promote compaction at heterochromatic regions (Bourguet et al., 2021). However, H2A.W was found to antagonize rather than promote H1 deposition at heterochromatin. Therefore, the features that drive H1 to preferentially incorporate into heterochromatin are yet to be discovered.

Methods

Plant materials and growth conditions

Arabidopsis thaliana plants in this study were Col-0 ecotype and were grown under 16h light: 8h dark condition (on soil), or under constant light (on plates). The following plant materials were used: wild-type (WT, non-transgenic), *h1* (double homozygous mutant consisting of, *h1.1-1* [SALK_128430] and *h1.2–1* [GABI_406H11], originally described by (Zemach et al., 2013)), *nrpe1* (*nrpe1-11* [SALK_029919]), ZF-DMS3 (this is a homozygous transgenic line containing the pEG302-DMS3-3xFLAG-ZF construct in Col-0 WT, originally described by (Gallego-bartolome et al., 2019)), SUVH1-3xFLAG in *suvh1* (this is a complementing homozygous transgenic line containing the pEG302-gSUVH1-3xFLAG construct in *suvh1-1*, originally described by (Harris et al., 2018)), SUVH1-3xFLAG in *h1* (this line was generated for this work, by transforming the same pEG302-gSUVH1-3xFLAG construct into the *h1.1-1* [SALK_128430] and *h1.2–1* [GABI_406H11] double mutant background), and the *h1*/*nrpe1* CRISPR lines (described below).

Generation of CRISPR lines

Two independent NRPE1 knockout lines were generated in the background of *h1* (*h1.1-1 h1.2-1* double, see above), designated as *h1/nrpe1* cKO_49 and *h1/nrpe1* cKO_63. The lines were generated using the previously published pYAO::hSpCas9 system (Yan et al., 2015) as described by (Ichino et al., 2021). Briefly, the two guides (ATTCTTGACGGAGAGATTGT, and TCTGGCACTGACAAACAGTT) targeting hSpCas9 to NRPE1 (AT2G40030) exons were sequentially cloned in the SpeI linearized pYAO::hSpCas9 construct by In-Fusion (Takara, cat #639650). The final vector was electroporated into AGL0 agrobacteria and transformed in *h1* mutant plants by agrobacterium-mediated floral dipping. T1 plants were selected on ½ MS agar plates with

hygromycin B and were PCR genotyped to identify plants with deletions spanning the guide region. Selected lines were taken to T2 and genotyped to identify those that had segregated out the pYAO::hSpCas9 transgene. Cas9 negative plants that were homozygous for an NRPE1 deletion (*h1/nrpe1* cKO_49) or an indel-induced frameshift to premature stop codon (*h1/nrpe1* cKO_63) were confirmed in the T3 generation (see Supplementary Fig. 4).

Chromatin immunoprecipitation sequencing (ChIP-seq) and western blot

All the material for ChIP used in this paper were from pooled 10-12 days old seedlings grown on Murashinge and Skoog agar plates (1/2X MS, 1.5% agar, pH5.7). The ChIP protocol used has been previously described (Ichino et al., 2021; Villar and Kohler, 2018), with minor modifications. Briefly, 2-4g of seedling tissue was used for each sample. Samples were ground in liquid nitrogen and crosslinked for 10 or 12 minutes at room temperature in Nuclei Isolation buffer (50mM Hepes pH8, 1M sucrose, 5mM KCl, 5mM MgCl2, 0.6% triton X-100, 0.4mM PMSF, 5mM benzamidine hydrochloride, cOmplete EDTA-free Protease Inhibitor Cocktail (Roche)) containing 1% formaldehyde. The crosslinking reactions were stopped with 125mM glycine by incubation at room temperature for 10 minutes. Crosslinked nuclei were filtered through one layer of miracloth, washed with Extraction Buffer 2, centrifuged through a layer of Extraction Buffer 3 and lysed with Nuclei lysis buffer (buffer compositions are described in the published protocol (Villar and Kohler, 2018)). Chromatin was sheared using a Bioruptor Plus (Diagenode) (20 cycles of 30 seconds on and 30 seconds off) and immunoprecipitated overnight at 4°C with antibody. anti-NRPE1 (endogenous antibody, described in (Liu et al., 2018)), anti-H1 (Agrisera, AS11 1801), anti-H3K9me2 (abcam, 1220), anti-H3 (abcam, 1791), anti-FLAG (for both the SUVH1-3xFLAG and the DMS3-ZF ChIPs, we used Anti-FLAG M2 (Sigma, F1804)). 25µl each of Protein A and Protein G magnetic Dynabeads (Invitrogen) were added to each sample and incubated for 2 more hours at 4°C. The immunoprecipitated chromatin was washed with Low Salt (2X), High Salt, LiCl and TE buffers, for 5 minutes each at 4°C (buffer compositions are described in the published protocol (Villar and Kohler, 2018)) and eluted twice with 250µl of elution buffer (1% SDS and 0.1M NaHCO3) in a thermomixer at 65°C and 1000 rpm, 20 minutes for each elution. Reverse crosslinking was performed overnight at 65°C in 0.2M NaCl, and proteins were degraded by proteinase K treatment at 45°C for 5h. The DNA fragments were purified using phenol:chloroform and ethanol precipitated overnight at −20°C. Libraries were prepared using the Ovation Ultralow System V2 kit (NuGEN, 0344NB-A01) following the manufacturer's instructions, with 15 cycles of PCR. Libraries were sequenced on a HiSeq 4000 or NovaSeq 6000 instrument (Illumina) using either single- or paired-end 50bp reads.

For the western blot shown in Supplementary Fig. 3A, 100ul of sheared chromatin was used as the input material for SDS-PAGE (as previously described (Harris et al., 2016)), using the anti-NRPE1 and anti-H1 antibodies described above.

ChIP-seq data analysis

ChIP-seq data were aligned to the TAIR10 reference genome with Bowtie2 (v2.1.0) (Langmead and Salzberg, 2012) allowing only uniquely mapping reads with zero mismatch. Duplicated reads were removed by Samtools. ChIP-seq peaks were called by MACS2 (v2.1.1) and annotated with ChIPseeker (Yu et al., 2015). Bigwig tracks were generated using the deepTools (v2.5.1) (Ramírez et al., 2016) bamCompare function, with samples scaled by mapped read count (--scaleFactorsMethod readCount) prior to log2 ratio or subtraction normalisation against corresponding input (Liu et al., 2018) or control samples. These tracks were used to generate metaplots using the computeMatrix and plotProfile / plotHeatmap functions in deepTools. Differential peaks were called by bdgdiff function in MACS2 (Zhang et al., 2008).

Whole-genome bisulfite sequencing (BS-seq) library preparation

Whole genome bisulfite sequencing libraries were generated as previously described (Harris et al., 2016), with minor modifications. The DNeasy Plant Mini Kit (Qiagen #69104) was used to isolate genomic DNA. 150µg of genomic DNA was used as input, a Covais S2 instrument was used for shearing (2 minutes), the Epitect Kit (QIAGEN #59104) was used for bisulfite conversion, and the Ultralow Methyl Kit (NuGEN) was used for library preparation and paired-end libraries were sequenced on a NovaSeq 6000 instrument.

Whole-genome bisulfite sequencing (BS-seq) data analysis

Previously published whole-genome bisulfite sequencing data for mutants and wild type were reanalyzed from previous paper (Stroud et al., 2013). Briefly, Trim_galore (*http://www.bioinformatics.babraham.ac.uk/projects/trim_galore/*) was used to trim adapters. BS-seq reads were aligned to TAIR10 reference genome by BSMAP (v2.90) and allowed 2 mismatches and 1 best hit (-v 2 -w 1) (Xi and Li, 2009). Reads with three or more consecutive CHH sites were considered as unconverted reads and filtered. DNA methylation levels were defined as #mC/ (#mC + #unmC). DMR overlapping analysis were conducted by mergePeaks (-d 100) of Homer (Heinz et al., 2010) with WGBS data published previously (Stroud et al., 2013). The estimated conversion rates for all WGBS libraries are provided in Supplementary Table 2.

Data and code availability

Data supporting the findings of this work are available within the paper and its Supplementary Information files. All high-throughput sequencing data generated in this study are accessible at NCBI's Gene Expression Omnibus (GEO) via GEO Series accession number GSE225480 (*https://www.ncbi.nlm.nih.gov/geo/query/acc.cgi?acc=GSE225480*). The pipelines and codes for downstream analysis are available on GitHub (*https://github.com/Zhenhuiz/H1-restricts-euchromatin-associated-methylation-pathways-from-heterochromatic-encroachment*). The bed files used to generate to plots are supplied in Supplementary Table 3.

Acknowledgements

We thank Mahnaz Akhavan for support with high-throughput sequencing at the UCLA Broad Stem Cell Research Center BioSequencing Core Facility. C.J.H is supported by a Royal Society University Research Fellowship (URF\R1\201016). This work was supported by NIH R35 GM130272 to S.E.J.. S.E.J is an Investigator of the Howard Hughes Medical Institute.

Author contributions

C.J.H. and S.E.J. designed the research. C.J.H., Z.Z. and S.E.J. wrote the manuscript. L.I. helped to isolate the *h1/nrpe1* CRISPR knockout lines. S.F. generated the WGBS libraries from genomic DNA. C.J.H. performed all other experiments. Z.Z. and C.J.H. performed the bioinformatic analyses.

References

Bednar J *et al.* (2017) **Structure and Dynamics of a 197 bp Nucleosome in Complex with Linker Histone H1** *Mol Cell* **66**:384–397 https://doi.org/10.1016/j.molcel.2017.04.012

Bohmdorfer G, Sethuraman S, Jordan Rowley M, Krzyszton M, Hafiz Rothi M, Bouzit L, Wierzbicki AT (2016) **Long non-coding RNA produced by RNA polymerase V determines boundaries of heterochromatin** *Elife* **5**:1–24 https://doi.org/10.7554/eLife.19092

Bourguet P *et al.* (2021) **The histone variant H2A.W and linker histone H1 co-regulate heterochromatin accessibility and DNA methylation** *Nat Commun* **12**:1–12 https://doi.org/10.1038/s41467-021-22993-5

Bourque G *et al.* (2018) **Ten things you should know about transposable elements 06 Biological Sciences 0604 Genetics** *Genome Biol* **19**:1–12 https://doi.org/10.1186/s13059-018-1577-z

Choi J, Lyons DB, Kim MY, Moore JD, Zilberman D (2020) **DNA Methylation and Histone H1 Jointly Repress Transposable Elements and Aberrant Intragenic Transcripts** *Mol Cell* **77**:310–323 https://doi.org/10.1016/j.molcel.2019.10.011

Choi J, Lyons DB, Zilberman D (2021) **Histone H1 prevents non-CG methylation-mediated small RNA biogenesis in Arabidopsis heterochromatin** *Elife* **10**:1–24 https://doi.org/10.7554/eLife.72676

Cuerda-Gil D, Slotkin RK (2016) **Non-canonical RNA-directed DNA methylation** *Nat Plants* **2** https://doi.org/10.1038/nplants.2016.163

Du J *et al.* (2014) **Mechanism of DNA methylation-directed histone methylation by KRYPTONITE** *Mol Cell* **55**:495–504 https://doi.org/10.1016/j.molcel.2014.06.009

Du J, Johnson LM, Jacobsen SE, Patel DJ. (2015) **DNA methylation pathways and their crosstalk with histone methylation** *Nat Rev Mol Cell Biol* **16**:519–532 https://doi.org/10.1038/nrm4043

Du J *et al.* (2012) **Dual binding of chromomethylase domains to H3K9me2-containing nucleosomes directs DNA methylation in plants** *Cell* **151**:167–80 https://doi.org/10.1016/j.cell.2012.07.034

Erdmann RM, Picard CL (2020) **RNA-directed DNA Methylation** *PLoS Genetics* https://doi.org/10.1371/journal.pgen.1009034

Gallego-bartolome J *et al.* (2019) **Co-targeting RNA Polymerases IV and V Promotes and V Promotes Efficient De Novo DNA Methylation in Arabidopsis** *Cell* **176**:1–15 https://doi.org/10.1016/j.cell.2019.01.029

Gibson BA, Doolittle LK, Schneider MWG, Jensen LE, Gamarra N, Henry L, Gerlich DW, Redding S, Rosen MK (2019) **Organization of Chromatin by Intrinsic and Regulated Phase Separation** *Cell* **179**:470–484 https://doi.org/10.1016/j.cell.2019.08.037

Harris CJ *et al.* (2016) **Arabidopsis AtMORC4 and AtMORC7 Form Nuclear Bodies and Repress a Large Number of Protein-Coding Genes** *PLOS Genet* **12** https://doi.org/10.1371/journal.pgen.1005998

Harris CJ *et al.* (2018) **A DNA methylation reader complex that enhances gene transcription** *Science* **362**:1182–1186

He S, Vickers M, Zhang J, Feng X (2019) **Natural depletion of histone H1 in sex cells causes DNA demethylation, heterochromatin decondensation and transposon activation** *Elife* **8**:1–23 https://doi.org/10.7554/ELIFE.42530

He S, Yu Y, Wang L, Zhang J, Bai Z, Li G, Li P, Feng X (2024) **Linker histone H1 drives heterochromatin condensation via phase separation in Arabidopsis** *Plant Cell* https://doi.org/10.1093/plcell/koae034

Heinz S, Benner C, Spann N, Bertolino E, Lin YC, Laslo P, Cheng JX, Murre C, Singh H, Glass CK (2010) **Simple Combinations of Lineage-Determining Transcription Factors Prime cis-Regulatory Elements Required for Macrophage and B Cell Identities** *Mol Cell* **38**:576–589 https://doi.org/10.1016/j.molcel.2010.05.004

Ichino L, Boone BA, Strauskulage L, Harris CJ, Kaur G, Gladstone MA, Tan M, Feng S, Jami-alahmadi Y, Duttke SH (2021) **MBD5 and MBD6 couple DNA methylation to gene silencing through the J-domain protein SILENZIO** *Science (80-)* **1439**:1434–1439

Johnson LM *et al.* (2014) **SRA- and SET-domain-containing proteins link RNA polymerase V occupancy to DNA methylation** *Nature* **507**:124–128 https://doi.org/10.1038/nature12931

Langmead B, Salzberg SL (2012) **Fast gapped-read alignment with Bowtie 2** *Nat Methods* **9**:357–359 https://doi.org/10.1038/nmeth.1923

Law J a, Du J, Hale CJ, Feng S, Krajewski K, Palanca AMS, Strahl BD, Patel DJ, Jacobsen SE. (2013) **Polymerase IV occupancy at RNA-directed DNA methylation sites requires SHH1** *Nature* **498**:385–389 https://doi.org/10.1038/nature12178

Li X, Harris CJ, Zhong Z, Chen W, Liu R, Jia B, Wang Z, Li S, Jacobsen SE, Du J. (2018) **Mechanistic insights into plant SUVH family H3K9 methyltransferases and their binding to context-biased non-CG DNA methylation** *PNAS* :1–10 https://doi.org/10.1073/pnas.1809841115

Liu W *et al.* (2018) **RNA-directed DNA methylation involves co-transcriptional small-RNA-guided slicing of polymerase v transcripts in Arabidopsis** *Nat Plants* **4**:181–188 https://doi.org/10.1038/s41477-017-0100-y

Liu Y, Zhang Z, Hu H, Chen W, Zhang F, Wang Q, Wang C, Yan K, Du J. (2024) **Molecular basis of chromatin remodelling by DDM1 involved in plant DNA methylation** *Nat Plants* https://doi.org/10.1038/s41477-024-01640-z

Matzke M a., Mosher R a. (2014) **RNA-directed DNA methylation: an epigenetic pathway of increasing complexity** *Nat Rev Genet* **15**:394–408 https://doi.org/10.1038/nrg3683

Osakabe A *et al.* (2021) **The chromatin remodeler DDM1 prevents transposon mobility through deposition of histone variant H2A.W** *Nat Cell Biol* **23**:391–400 https://doi.org/10.1038/s41556-021-00658-1

Panda K, Ji L, Neumann DA, Daron J, Schmitz RJ, Slotkin RK (2016) **Full-length autonomous transposable elements are preferentially targeted by expression-dependent forms of RNA-directed DNA methylation** *Genome Biol* **17** https://doi.org/10.1186/s13059-016-1032-y

Papareddy RK, Páldi K, Paulraj S, Kao P, Lutzmayer S, Nodine MD (2020) **Chromatin regulates expression of small RNAs to help maintain transposon methylome homeostasis in Arabidopsis** *Genome Biol* **21** https://doi.org/10.1186/s13059-020-02163-4

Ramírez F, Ryan DP, Grüning B, Bhardwaj V, Kilpert F, Richter AS, Heyne S, Dündar F, Manke T (2016) **deepTools2: a next generation web server for deep-sequencing data analysis** *Nucleic Acids Res* **44**:W160–W165 https://doi.org/10.1093/nar/gkw257

Ruiz-Velasco M, Zaugg JB (2017) **Structure meets function: How chromatin organisation conveys functionality** *Curr Opin Syst Biol* **1**:129–136 https://doi.org/10.1016/j.coisb.2017.01.003

Rutowicz K *et al.* (2019) **Linker histones are fine-scale chromatin architects modulating developmental decisions in Arabidopsis** *Genome Biol* **20**:1–22 https://doi.org/10.1186/s13059-019-1767-3

Saha A, Dalal Y (2021) **A glitch in the snitch: The role of linker histone H1 in shaping the epigenome in normal and diseased cells** *Open Biol* **11** https://doi.org/10.1098/rsob.210124

Sigman MJ, Panda K, Kirchner R, McLain LL, Payne H, Peasari JR, Husbands AY, Slotkin RK, McCue AD (2021) **An siRNA-guided ARGONAUTE protein directs RNA polymerase V to initiate DNA methylation** *Nat Plants* **7**:1461–1474 https://doi.org/10.1038/s41477-021-01008-7

Stroud H, Do T, Du J, Zhong X, Feng S, Johnson L, Patel DJ, Jacobsen SE. (2014) **Non-CG methylation patterns shape the epigenetic landscape in Arabidopsis** *Nat Struct Mol Biol* **21**:64–72 https://doi.org/10.1038/nsmb.2735

Stroud H, Greenberg MVC, Feng S, Bernatavichute Y V, Jacobsen SE (2013) **Comprehensive Analysis of Silencing Mutants Reveals Complex Regulation of the Arabidopsis Methylome** *Cell* **152**:352–364 https://doi.org/10.1016/j.cell.2012.10.054

Teano G *et al.* (2023) **Histone H1 protects telomeric repeats from H3K27me3 invasion in Arabidopsis** *Cell Rep* **42** https://doi.org/10.1016/j.celrep.2023.112894

Villar CBR, Kohler C (2018) **Plant Chromatin immunoprecipitation** *Methods Mol Biol* **1839**:65–75 https://doi.org/10.1007/978-1-4939-8685-9_7

Wang Z, Baulcombe DC (2020) **Transposon age and non-CG methylation** *Nat Commun* **11**:1–9 https://doi.org/10.1038/s41467-020-14995-6

Wierzbicki AT, Haag JR, Pikaard CS (2008) **Noncoding Transcription by RNA Polymerase Pol IVb/Pol V Mediates Transcriptional Silencing of Overlapping and Adjacent Genes** *Cell* **135**:635–648 https://doi.org/10.1016/j.cell.2008.09.035

Wierzbicki AT, Ream TS, Haag JR, Pikaard CS (2009) **RNA polymerase V transcription guides ARGONAUTE4 to chromatin** *Nat Genet* **41**:630–4 https://doi.org/10.1038/ng.365

Wongpalee SP *et al.* (2019) **CryoEM structures of Arabidopsis DDR complexes involved in RNA-directed DNA methylation** *Nat Commun* **10**:1–12 https://doi.org/10.1038/s41467-019-11759-9

Xi Y, Li W (2009) **BSMAP: Whole genome bisulfite sequence MAPping program** *BMC Bioinformatics* **10**:1–9 https://doi.org/10.1186/1471-2105-10-232

Yan L, Wei S, Wu Y, Hu R, Li H, Yang W, Xie Q (2015) **High-Efficiency Genome Editing in Arabidopsis Using YAO Promoter-Driven CRISPR/Cas9 System** *Mol Plant* **8**:1820–1823 https://doi.org/10.1016/j.molp.2015.10.004

Yu G, Wang LG, He QY (2015) **ChIP seeker: An R/Bioconductor package for ChIP peak annotation, comparison and visualization** *Bioinformatics* **31**:2382–2383 https://doi.org/10.1093/bioinformatics/btv145

Zemach A, Kim MY, Hsieh P-H, Coleman-Derr D, Eshed-Williams L, Thao K, Harmer SL, Zilberman D (2013) **The Arabidopsis nucleosome remodeler DDM1 allows DNA methyltransferases to access H1-containing heterochromatin** *Cell* **153**:193–205 https://doi.org/10.1016/j.cell.2013.02.033

Zhang Y *et al.* (2018) **Large-scale comparative epigenomics reveals hierarchical regulation of non-CG methylation in Arabidopsis** *Proc Natl Acad Sci* **201716300** https://doi.org/10.1073/pnas.1716300115

Zhang Y *et al.* (2008) **Model-based analysis of ChIP-Seq (MACS)** *Genome Biol* **9** https://doi.org/10.1186/gb-2008-9-9-r137

Zhong X, Du J, Hale CJ, Gallego-Bartolome J, Feng S, Vashisht AA, Chory J, Wohlschlegel JA, Patel DJ, Jacobsen SE. (2014) **Molecular Mechanism of Action of Plant DRM De Novo DNA Methyltransferases** *Cell* **157**:1050–1060 https://doi.org/10.1016/j.cell.2014.03.056

Zhong X, Hale CJ, Law JA, Johnson LM, Feng S, Tu A, Jacobsen SE (2012) **DDR complex facilitates global association of RNA polymerase V to promoters and evolutionarily young transposons** *Nat Struct Mol Biol* **19**:870–5 https://doi.org/10.1038/nsmb.2354

Article and author information

C. Jake Harris

Department of Molecular, Cell and Developmental Biology, University of California, Los Angeles, CA, USA, Department of Plant Sciences, University of Cambridge, Cambridge CB2 3EA, UK

For correspondence: cjh92@cam.ac.uk

ORCID iD: 0000-0001-5120-0377

Zhenhui Zhong

Department of Molecular, Cell and Developmental Biology, University of California, Los Angeles, CA, USA, Ministry of Education Key Laboratory for Bio-Resource and Eco-Environment, College of Life Sciences, Sichuan University, Chengdu 610065, China

Lucia Ichino

Department of Molecular, Cell and Developmental Biology, University of California, Los Angeles, CA, USA

Suhua Feng
Department of Molecular, Cell and Developmental Biology, University of California, Los Angeles, CA, USA, Eli & Edythe Broad Center of Regenerative Medicine & Stem Cell Research, University of California, Los Angeles, Los Angeles, CA, USA

Steven E. Jacobsen
Department of Molecular, Cell and Developmental Biology, University of California, Los Angeles, CA, USA, Eli & Edythe Broad Center of Regenerative Medicine & Stem Cell Research, University of California, Los Angeles, Los Angeles, CA, USA, Howard Hughes Medical Institute, University of California, Los Angeles, CA, USA
For correspondence: jacobsen@ucla.edu

Copyright

Editors

Reviewing Editor
Richard Amasino
University of Wisconsin Madison, Madison, United States of America

Senior Editor
Detlef Weigel
Max Planck Institute for Biology Tübingen, Tübingen, Germany

Reviewer #1 (Public Review):

In this study, the authors obtained multiple, novel and compelling datasets to better understand the relationship between histone H1 and RNA-directed DNA methylation in plants. Most of the authors' claims concerning H1 and RNA polymerase V (Pol V) are backed by convincing and independent lines of evidence. However, Pol V produces noncoding transcripts that act as scaffold RNAs, which AGO4-bound siRNAs recognize in plant chromatin to mediate RNA-directed DNA methylation. Detection of Pol V transcript products at the sites of Pol V redistribution in h1 mutants would significantly enhance the impact of this manuscript. Below I have listed several strengths and a weakness of the manuscript.

Strengths:

- The authors report high-quality NRPE1 ChIP-seq data, allowing them to directly test how and where Pol V occupancy depends on histone H1 function in Arabidopsis.
- nrpe1 mutants generated via CRISPR/Cas9 in the h1 mutant background (nrpe1 h1.1-1 h1.2-1 triple mutants), allow the authors to study the role of Pol V in ectopic DNA methylation in H1-deficient plants.
- Pol V recruitment via ZincFinger-DMS3 expression (a modified version of Pol V's DMS3 recruitment factor) sends Pol V to new genomic loci and thus provides the authors with an innovative dataset for understanding H1 function at these sites.

Weakness:

- The manuscript does not include detection or quantification of Pol V transcripts generated at ectopic sites in the h1 mutant background. Pol V encroachment into heterochromatin in the h1 mutant is indirectly shown by NRPE1-dependent methylation at such ectopic sites.

Previous studies have charted the relationship between H1 function and RNA-directed DNA methylation (RdDM) via analyses of Pol IV-dependent 24 nt siRNAs and factors that recruit Pol IV (Choi et al., 2021 and Papareddy et al., 2020). Harris and colleagues have extended this work and shown that histone H1 function also antagonizes Pol V occupancy in the context of constitutive heterochromatin. The authors thus provide important evidence to show that H1 limits the encroachment of both polymerases Pol IV and Pol V into plant heterochromatin.

https://doi.org/10.7554/eLife.89353.2.sa1

Reviewer #2 (Public Review):

Summary:

The main conclusion of the manuscript is that the presence of linker Histone H1 protects Arabidopsis pericentromeric heterochromatic regions and longer transposable elements from encroachment by other repressive pathways. The manuscript focuses on the RNA-dependent DNA-methylation (RdDM) pathway but indirectly finds that other pathways must also be ectopically enriched.

Strengths:

The authors present diverse sets of genomic data comparing Arabidopsis wild-type and h1 mutant background allowing an analysis of differential recruitment of RdDM component NPRE1, which is related to changes in DNA methylation and H1 coverage. The manuscript also contains recruitment data for SUVH1 in wild-type and h1 mutant backgrounds. Furthermore, the authors make use of a line that recruits NRPE1 ectopically to show that H1 occupancy is not altered because of this recruitment. These data clearly show that there is a hierarchy in which DNA-methylation is impacted by presence of H1 while H1 distribution is independent of DNA-methylation.

Weaknesses:

The manuscript is driven by a strong and reasonable hypothesis that absence of H1 results increased access of chromatin binding factors and that this explains how the RdDM machinery is restricted from encroaching heterochromatic regions, which are particularly enriched in H1. Indeed, increased binding of NPRE1 at pericentromeric sites is observed; however, the major DNA-methylation changes at these sites are symmetric and not related to the RdDM pathway. Thus, the authors propose that many factors redistribute, which is again reasonable. The authors show redistribution of SUVH1 and relate their data to a previous report showing redistribution of the PcG machinery in H1 depletion mutants (Teano et al. in Cell reports (Volume 42, Issue 8, 29 August 2023), but the manuscript provides limited mechanistic insight as to why there is a strong increase in heterochromatin symmetric DNA-methylation.

https://doi.org/10.7554/eLife.89353.2.sa0

Author response:

The following is the authors' response to the original reviews.

Recommendations for the authors:

Reviewer #1 (Recommendations For The Authors):

> *Pg. 3 - lines 51-53: "Once established, the canonical RdDM pathway takes over, whereby small RNAs are generated by the plant-specific polymerase IV (Pol IV). In both cases, a second plant-specific polymerase, Pol V, is an essential downstream component." The authors' intro omits an important aspect of Pol V's function in RdDM, which is quite relevant to their study. Pol V transcribes DNA to synthesize noncoding RNA scaffolds, to which AGO4-bound 24 nt siRNAs are thought to base pair, leading to DRM2 recruitment for cytosine methylation near to these nascent Pol V transcripts (Wierzbicki et al 2008 Cell; Wierzbicki et al. 2009 Nat Genet). I recommend that the authors cite these key studies.*

These citations have now been added (see line 57).

> *The authors provide compelling evidence that Pol V redistributes to ectopic heterochromatin regions in h1 mutants (e.g., Fig1a browser shot). Presumably, this would allow Pol V to transcribe these regions in h1 mutants, whereas it could not transcribe them in WT plants. Have the authors detected and/or quantified Pol V transcripts in the h1 mutant compared to WT plants at the sites of Pol V redistribution (detected via NRPE1 ChIP)?*

Robust detection of Pol V transcripts can be experimentally challenging, and instead we quantify and detect NRPE1 dependent methylation at these regions (Fig 5), which occurs downstream of Pol V transcript production. However, we note detecting Pol V transcripts as a potential future direction in the discussion (see line 263).

> *Pg. 5 - lines 101-102: Figure 1e - "The preferential enrichment of NRPE1 in h1 was more pronounced at TEs that overlapped with heterochromatin associated mark, H3K9me2 (Fig. 1e). Was a statistical test performed to determine that the overall differences are significant only at TE sites with H3K9me2? Can the sites without H3K9me2 also be differentiated statistically?*

Yes, there is a statistically significant difference between WT and h1 at both the H3K9me2 marked and unmarked TEs (Wilcoxon rank sum tests, see updated Fig 1e). The size of the effect is larger for the H3K9me2 marked TEs (median difference of 0.41 vs 0.16). Median values have now been added to the boxplots so that this is directly viewable to the reader (Fig 1e). This reflects the general increase in NRPE1 occupancy in *h1* mutants through the genome, with the effect consistently stronger in heterochromatin. In our initial version of the manuscript, we summarise the effect as follows “We found that h1 antagonizes NRPE1 occupancy throughout the genome, particularly at heterochromatic regions” (previous version line 83, current version line 95). Although important exceptions exist (see Fig 5, NRPE1 and DNA methylation loss in h1), we now make this point even more explicit, and have updated the manuscript at several locations (abstract line 26, results line 245, discussion line 265).

> *Pg. 5 - lines 108-110: The authors state, "Importantly, we found no evidence for increased NRPE1 expression at the mRNA or protein level in the h1 mutant (Suppl. Fig. 2)." But the authors did observe reduced NRPE1 transcript levels in h1 mutants, in their re-analysis of RNA-seq data and reduced NRPE1 protein signals via western blot in (Suppl. Fig. 2), which should be reported here in the results.*

As described further below, we reanalysed *h1* RNA-seq from scratch, and see no evidence for significant differential gene expression of NRPE1. This table and analysis are now provided in Supplementary Table 1.

> *More importantly, the above logic about NRPE1 expression in h1 mutants assumes that NRPE1 is the stoichiometrically limiting subunit for Pol V assembly and function in vivo, but this is not known to be the case:*
>
> *(1) While NRPE1's expression is somewhat reduced (and not increased) in h1 mutant plants, we cannot be certain that other genes influencing Pol V stability or recruitment are unaffected by h1 mutants. I thus recommend that the authors perform RT-qPCR directly on the WT and h1 mutant materials used in their current study, quantifying NRPE1, NRPE2, NRPE5, DRD1, DMS3, RDM1, SUVH2 and SUVH9 transcript levels.*
>
> *(2) Normalizations used to compare samples should be included with RT-qPCR and western assays. An appropriate house-keeping gene like Actin2 or Ubiquitin could be used to normalize the RT-qPCR. Protein sample loading in Suppl. Fig. 2 could be checked by Coomassie staining and/or an antibody detection of a house-keeping protein.*

We have now included a full re-analysis of *h1* RNA-seq (data from Choi et al 2020) focusing on transcriptional changes of DNA methylation machinery genes in the *h1* mutant. Of the 61 genes analysed, only AGO6 and AGO9 were found to be differentially expressed (2-3 fold upregulation). This analysis is now included as a table

(Supplementary Table 1). The western blot has been moved to Supplementary Fig 3 to now illustrate antibody specificity and H1 loss in the *h1* mutant lines, so NRPE1 itself serves as a loading control (Supplementary Fig 3a).

> *Pg. 6 - lines 129-131: The authors state that "over NRPE1 defined peaks (where NRPE1 occupancy is strongest in WT) we observed no change in H1 occupancy in nrpe1 (Fig 2b). The results indicate that H1 does not invade RdDM regions in the nrpe1 mutant background." This conclusion assumes that the author's H1 ChIP is successfully detecting H1 occupancy. However, in Fig 2d there does not appear to be H1 enrichment or peaks as visualized across the 10766 ZF-DMS3 off-target loci, or even at the selected 451 ZFDMS3 off-target hyper DMRs, where the putative signal for H1 enrichment on the metaplot center is extremely weak/non-existent.*
>
> *As a reference for H1 enrichment in chromatin (e.g., looking where H2A.W antagonizes H1 occupancy) one can compare analyses in Bourguet et al (2021) Nat Commun, involving co-authors of the current study. Bourguet et al (2021) Fig 5b show a metaplot of H1 levels centered on H2A.W peaks with H1 ChIP signal clearly tapering away from the metaplot center point peak. To my eye, the H1 ChIP metaplots for ZF-DMS3 offtarget loci in the current manuscript (Fig 2d) resemble "shuffled peaks" controls like those in Fig 5b of Bourguet et al (2021).*
>
> *Can one definitively interpret Fig 2d as showing RdDM "not reciprocally affecting H1 localization" without first showing the specificity of the ChIP-seq results in a genotype where H1 occupancy changes? Alternatively, could this dataset be displayed with Deeptools heatmaps to strengthen the evidence that the authors are detecting H1 occupancy/enrichment genome-wide, before diving into WT/nrpe1 mutant analysis at ZF-DMS3 off-target loci?*

This is an excellent suggestion from the reviewer. We have now included several analyses that assess and demonstrate the quality of our H1 ChIP-seq profiles. First, as suggested by the reviewer, we show that our H1 profiles peak over H2A.W enriched euchromatic TEs as

defined by Bourguet et al, mirroring these published findings. Next, we investigated whether our H1 profiles match Teano's recently described pattern over genes, confirming a similar pattern with 3' enrichment of H1 over H3K27me3 unmarked genes. Furthermore, we show that the H1 peaks defined here are similarly enriched with GFP tagged H1.2 from the Teano et al. 2023 study. These analyses that validate the quality of our H1 ChIP-seq datasets and bolster the conclusion that NRPE1 redistribution does not affect H1 occupancy. These new analysis are now presented in Supplementary Figure 3 and see line 153.

> *Pg. 8 - lines 228-230: The authors state that, "As with NRPE1, SUVH1 increased in the h1 background significantly more in heterochromatin, with preferential enrichment over long TEs, cmt2 dependent hypo CHH DMRs, and heterochromatic TEs (Fig. 6b)."*
>
> *Contrary to the above statement, the violin plots in Fig. 6c show SUVH1 occupancy increasing at euchromatic TEs in the h1 mutant. What statistical test allowed the authors to determine that the increase in h1 occurs "significantly more in heterochromatin"? The authors should critically interpret Fig. 6c and 6d, which are not currently referenced in the results section. More support is needed for the claim that SUVH1 specifically encroaches into heterochromatin in the h1 mutant, rather than just TEs generally (euchromatic and heterochromatic alike).*

Similar to what we see for NRPE1, statistical tests that we have now performed show that SUVH1 is significantly enriched in h1 in all classes. Importantly however, the effect size is larger in all of the heterochromatin associated classes. We display these statistical tests and the median values on the plots so that effects are immediately viewable (see updated Fig 6).

> *In addition, the authors should verify that SUVH1-3xFLAG transgenes (in the WT and h1 mutant backgrounds, respectively) and endogenous Arabidopsis genes encoding the transcriptional activator complex (SUVH1-SUVH3-DNAJ1-DNAJ2) are not overexpressed in the h1 mutant vs. WT. Higher expression of SUVH1 or limiting factors in the larger complex could explain the observation of increased SUVH1 occupancy in the h1 background.*

We do not see a difference in SUVH1/3/DNAJ1/2 complex gene expression in the *h1* background (see Supplementary Table 1). However, we cannot rule out that that our SUVH1-FLAG line in *h1* is more highly expressed than the corresponding SUVH1-FLAG line in WT. We now note this point in line 248.

> *Pg. 8 - lines 231-232: Here the authors make a sweeping conclusion about H1 demarcating, "the boundary between euchromatic and heterochromatic methylation pathways, likely through promoting nucleosome compaction and restricting heterochromatin access." I do not see how a H1 boundary between euchromatic and heterochromatic methylation pathways is revealed based on the SUVH1-3xFLAG occupancy data, which shows increased enrichment at every category interrogated in the h1 mutant (Fig 6b,c,d) and all along the baseline too in the h1 mutant browser tracks (Fig 6a). Can the authors provide more examples of this phenomenon (similar to Fig 6a) and better explain why their SUVH1-3xFLAG ChIP supports this demarcation model?*

The general conclusion from SUVH1 about H1's agnostic role in preventing heterochromatin access is now further supported from our findings with H3K27me3 (see Figure 6e and description from line 250). However, we agree that the demarcation model as initially presented was overly simplistic. This point was also raised by reviewer 2. We have removed the line highlighted by the reviewer in the revised version of the manuscript. In the revised version we clarify that H1 impedes RdDM and associated machinery throughout the genome (consistent with H1's established broad occupancy across the genome) but this effect is most

pronounced in heterochromatin, corresponding to maximal H1 occupancy (abstract line 26, results line 245, discussion line 265).

> *Corrections:*
>
> *Pg. 8 - lines 226-227: "We therefore wondered whether complex's occupancy might also be affected by H1." The sentence contains a typo, where I assume the authors mean to refer to occupancy by the SUVH1-SUVH3-DNAJ1-DNAJ2 transcriptional activator complex. This needs to be specified more clearly.*

The paragraph has been updated (see from line 237).

> *Pg. 13 - lines 393-405: There are minor errors in the capitalization of titles and author initials in the References. I recommend that the authors proofread all the references to eliminate these issues:*

Thank you, these have been corrected.

Choi J, Lyons DB, Zilberman D. 2021. Histone H1 prevents non-cg methylation-mediated small RNA biogenesis in arabidopsis heterochromatin. Elife 10:1-24. doi:10.7554/eLife.72676 (...)

Du J, Johnson LM, Groth M, Feng S, Hale CJ, Li S, Vashisht A a., Gallego-Bartolome J, Wohlschlegel J a., Patel DJ, Jacobsen SE. 2014. Mechanism of DNA methylation-directed histone methylation by KRYPTONITE. Mol Cell 55:495-504. doi:10.1016/j.molcel.2014.06.009 (...)

Du J, Zhong X, Bernatavichute Y V, Stroud H, Feng S, Caro E, Vashisht A a, Terragni J, Chin HG, Tu A, Hetzel J, Wohlschlegel J a, Pradhan S, Patel DJ, Jacobsen SE. 2012. Dual binding of chromomethylase domains to H3K9me2-containing nucleosomes directs DNA methylation in plants. Cell 151:167-80. doi:10.1016/j.cell.2012.07.034

> ***Reviewer #2 (Recommendations For The Authors):***
>
> *As for a normal review, here are our major and minor points.*
>
> *Major:*
>
> *(1) Lines 38 to 45 of the introduction are important for the subsequent definition of heterochromatic and non-heterochromatic transposons, but the definition is ambiguous. Is heterochromatin defined by surrounding context such as pericentromeric position or is this an autonomous definition? Can a TE with the chromosomal arms be considered heterochromatic provided that it is long enough and recruits the right machinery? These cases should be more explicitly introduced. Ideally, a supplemental dataset should provide a key to the categories, genomic locations and overlapping TEs as they were used in this analysis, even if some of the categories were taken from another study.*

We have now added all the regions used for analysis in this study to Supplementary Table 3.

> *(2) Line 80: This would be the first chance to cite Teno et al. and the "encroachment" of*

PcG complexes to TEs in H1 mutants

Done - “H1 also plays a key role in shaping nuclear architecture and preventing ectopic polycomb-mediated H3K27me3 deposition in telomeres (Teano et al., 2023).” See line 83

> *(3) It is "only" a supplemental figure but S2 but it should still follow the rules: Indicate the number of biological replicates for the RNA-seq data, and perform a statistical test. In case of WB data, provide a loading control.*

We are now using the western blot to illustrate antibody specificity and H1 loss in the *h1* mutant lines, so NRPE1 itself serves as a loading control (Supplementary Fig 3a). For NRPE1 mRNA expression, we have now replaced this with a more comprehensive transcriptome analysis of methylation machinery in *h1* (see Supplementary Table 1).

> *(4) Lines 115 to 124 and corresponding data: Here, the goal is to exclude other changes to heterochromatin structure other than "increased access" in H1 mutants; however, only one feature, H3K9me2, is tested. Testing this one mark does not necessarily prove that the nature of the chromatin does not change, e.g. H2A.W could be differently redistributed, DDM1 may change, VIM protein, and others. Either more comprehensive testing for heterochromatin markers should be performed, or the conclusions moderated.*

We have moderated the text accordingly (see line 135).

> *(5) Lines 166ff and Figure 1, a bit out of order also Figure 5: The general hypothesis is that NRPE1 redistributes to heterochromatic regions in h1 mutants (as do other chromatin modifiers), but the data seem to only support a higher occurrence at target sites.*
>
> *a. The way the NRPE1 data is displayed makes it seem like there is much more NRPE1 in the h1 samples, even at peaks that should not be recruiting more as they do not represent "long" TEs. It would be good to present more gbrowse shots of all peak classes.*

We now clarify that *h1* does result in a general increase of NRPE1 throughout the genome, but the effect is strongest at heterochromatin. In our initial version of the manuscript, we summarise the effect as follows “We found that h1 antagonizes NRPE1 occupancy throughout the genome, particularly at heterochromatic regions” (previous version line 83, current version line 95). We have modified the language at several locations throughout the manuscript to make this point more clearly (abstract line 26, results line 245, discussion line 265). We include several browser shots in Supp Fig. 8.

> *b. The data are "normalized" how exactly?*
>
> *c. One argument of observing "gaining" and "losing" peaks is that there is redistribution of NRPE1 from euchromatic to heterochromatic sites. There should be an analysis and figure to corroborate the point (e.g. by comparing FRIP values). Figure 1b shows lower NRPE1 signals at the TE flanking regions. This could reflect a redistribution or a flawed normalization procedure.*

The data are normalised using a standardised pipeline by log2 fold change over input, after scaling each sample by mapped read depth using the bamCompare function in deepTools. This is now described in detail in the Materials and Methods line 365, with full code and pipelines available from GitHub (https://github.com/Zhenhuiz/H1-restrictseuchromatin-associated-methylation-pathways-from-heterochromatic-encroachment).

> *d. Figure 1d and f show similar profiles comparing "long" and "short" TEs or "CMT2 dependent hypo-CHH" and "DRM2 dependent CHH". How do these categories relate to each other, how many fragments are redundant?*

The short vs long TEs were defined in Liu et al 2018 (doi: 10.1038/s41477-017-0100-y) and the DMRs were defined in Zhang et al. 2018 (DOI: 10.1073/pnas.1716300115). There is likely to be some degree of overlap between the categories, but numbers are very different (short TEs (n=820), long TEs (n=155), drm2 DMRs (n=5534), CMT (n=21784)) indicating that the different

categories are informative. We have now listed all the regions used for analysis in this study as in Supplementary Table 3.

> *e. The purpose of the data presented in Figure 1 b is to compare changes of NRPE1 association in H3K9me3 non-overlapping and overlapping TEs between wild-type and background, yet the figure splits the categories in two subpanels and does neither provide a fold-change number nor a statistical test of the comparison. As before, the figure does not really support the idea that NPRE1 somehow redistribute from its "normal" sites towards heterochromatin as both TE classes seem to show higher NRPE1 binding in h1 mutants.*

There is a statistically significant difference between WT and *h1* at both the H3K9me2 marked and unmarked TEs, however, the size of the effect is larger for the H3K9me2 marked TEs (median difference of 0.41 vs 0.16). Median values have now been added to the boxplots so that this is directly viewable to the reader (Fig 1e). Although important exceptions exist (see Fig 5 – regions that lose NRPE1 and DNA methylation), this reflects the general increase in NRPE1 occupancy in *h1* mutants throughput the genome, with a consistently stronger effect in heterochromatin. As noted above, we have updated the manuscript to make this point more clearly (abstract line 26, results line 245, discussion line 265).

> *f. Panel g is the only attempt to corroborate the redistribution towards heterochromatic regions, but at this scale, the apparent reduction of binding in the chromosome arms may be driven by off-peak differences and normalization problems between different ChIP samples with different signal-to-noise-ratio.*

We describe our normalisation and informatic pipeline in more detail in the Materials and Methods line 365. It is also important to note that the reduction is not only observed at the chromosomal level, but also at specific sites. We called differential peaks between WT and *h1* mutant. The "Regions that gain NRPE1 in h1" peaks are more enriched in heterochromatic regions, while " Regions that lose NRPE1 in h1" peaks are more enriched outside heterochromatic regions.

> *g. Figure 5: how many regions gain vs lose NRPE1 in h1 mutants? If the "redistribution causes loss" scenario applies, the numbers should overall be balanced but that does not seem the case. The loss case appears to be rather exceptional judging from the zigzagging meta-plot. Are these sites related to the sites taken over by PcG-mediated repression in h1 mutants?*

As described in line 222 (previous version of the manuscript line 206), there are 15,075 sites that gain and 1,859 sites that lose NRPE1 in *h1*. Comparing these sites to

H3K27me3 in the Teano et al. study was an excellent suggestion. We compared sites that gain NRPE1 to sites that gain H3K27me3 in *h1*, finding a statistically significant overlap (2.4 fold enrichment over expected, hypergeometric test p-value 2.1e-71). Reciprocally, sites that lose NRPE1 were significantly enriched for overlap with H3K27me3 loss regions (1.6 fold over expected, hypergeometric test p-value 1.4e-4). This indicates that RdDM and H3K27me3 patterning are similarly modulated by H1. To directly test this, we reanalysed the H3K27me3 ChIP-seq data from Teano et al., finding coincident gain and loss of H3K27me3 at sites that gain and lose NRPE1 in *h1*. These results are described from line 250 and in Fig 6e, which supports a general role for H1 in preventing heterochromatin encroachment.

> *(6) Lines 166ff and Figure 3: The data walk towards the scenario of pathway redistribution but actually find that RdDM plays a minor role overall as a substantial*

> *increase in heterochromatin regions occurs in all contexts and is largely independent of RdDM.*
>
> *a. How exactly are DNA-methylation data converted across regions to reach a fraction score from 0 to 1? There is no explanation in the legend for the methods that allow to recapitulate.*

We now explain our methods in full in the Materials and Methods and all the code for generating these has now been deposited on GitHub (https://github.com/Zhenhuiz/H1restricts-euchromatin-associated-methylation-pathways-from-heterochromaticencroachment). Briefly, BSMAP is used to calculate the number of reads that are methylated vs unmethylated on a per-cytosine basis across the genome. Next, the DNA methylation fraction in each region is calculated by adding all the methylation fractions per cytosine in a given window, and divided by the total number of cytosines in that same window (ie mC/(unmC+mC)) i.e. this is expressed as a fraction ranging from 0 to 1.

"0" indicates this region is not methylated, and "1" indicates this region is fully methylated (every cytosine is 100% methylated).

> *b. Kernel plots? These are slang for experts and should be better described. In addition, nothing is really concluded from these plots in the text, although they may be quite informative.*

Kernel density plots show the proportion of TEs that gain or lose methylation in a particular mutant, rather than the overall average as depicted in the methylation metaplots above. We now describe the kernel density plots in more detail in the Figure 3 legend.

> *(7) Figure 4: This could be a very interesting analysis if the reader could actually understand it.*
>
> *a. The legend is minimal. What is the meaning of hypo and hyper regions indicated to the right of Figure 4c?*
>
> *b. The color scale represents observed/expected values. What exactly does this mean? Mutant vs WT?*
>
> *c. Some comparisons in 4a are cryptic, e.g. h1 nrpe1 nrpe1 vs CHH?*
>
> *d. Figure 4d focuses on a correlation square of relevance, but why? Interestingly the square does not correspond to any "hypo" or "hyper" label?*

Thank you, we have revised Figure 4 and legend based on these suggestions to clarify all of the above.

> *(8) Lines 226 and Figure 6B. De novo (or increased) targeting of SUVH1 to heterochromatic sites in h1 mutants, similar to NRPE1, is used to support the argument that more access allows other chromatin modifiers to encroach. SUVH1 strongly depends on RdDM for its in vivo binding and may be the least conclusive factor to argue for a "general" encroachment mechanism.*

We appreciate the reviewers point here. Something that is entirely independent of RdDM following the same pattern would be stronger evidence in favour of general encroachment. Excitingly, this is exactly what we provide evidence for when investigating the interrelationship with H3K27me3 and we appreciate the reviewer's suggestion to check this! This data is now described in Figure 6e and line 250.

> *Minor:*
>
> *(1) Line 23: "Loss of H1 resulted in heterochromatic TE enrichment by NRPE1." This does not seem right. NRPE enrichment as TEs*

Modified, (line 26) thank you.

> *(2) Lines 73-74: The idea that DDM1 displaces H1 in heterochromatic TEs is somewhat counterintuitive to model that heterochromatic TEs are unavailable for RdDM because of the presence of H1. Is this displacement non-permanent and directly linked to interaction with CMT2/3 Met1?*

This is a very good question and we agree with the reviewer that the effect of DDM1 may only be transient or insufficient to allow for full RdDM assembly, or indeed there may be a direct interaction between DDM1 and CMTs/MET1. During preparation of these revisions, a structure of Arabidopsis nucleosome bound DDM1 was published, which provides some insight by showing that DDM1 promotes DNA sliding. This is at least consistent with the idea of DDM1 causing transient / non-permanent displacement of H1 that would be insufficient for RdDM establishment. We incorporate discussion of these ideas at line 80.

> *(3) Line 85: A bit more background on the Reader activator complex should be given. In fact, the reader may not really care that it was more recently discovered (not really recent btw) but what does it actually do?*

We have quite extensively reconfigured this paragraph to take into account our new finding with H3K27me3, such that there is less emphasis on the reader activator complex. The sentence now reads as follows:

“We found that h1 antagonizes NRPE1 occupancy throughout the genome, particularly at heterochromatic regions. This effect was not limited to RdDM, similarly impacting both the methylation reader complex component, SUVH1 (Harris et al., 2018) and polycomb-mediated H3K27me3 (Teano et al., 2023).” (line 95).

Also, when describing the experiment the results section (line 241), we now provide more background on SUVH1’s function.

> *(4) Lines 80-81: Since it is already shown that RdDM associated small RNAs are more enriched in h1 at heterochromatin, help us to know what is precisely the added value of studying the enrichment of NRPE1 at these sites.*

Good point. We have the following line: ‘...small RNAs are not a direct readout of functional RdDM activity and Pol IV dependent small RNAs are abundant in regions of the genome that do not require RdDM for methylation maintenance and that do not contain Pol V (Stroud et al., 2014).’ (line 90)

> *(5) Line 99: This seems to be the only time where the connection between long TEs and heterochromatic regions is mentioned but no source is cited.*

We have added the following appropriate citations: (Bourguet et al., 2021; Zemach et al., 2013). (line 110).

> *(6) Line 100: DMRs is used for the first time here without explanation and full text. The abbreviation is introduced later in the text (Line 187).*

Thank you, we now describe DMRs upon first use, line 112.

> *(7) Figure 2: Panels 2 c and d should show metaplots for WT and transgenes in one panel. There is something seriously wrong with the normalization in d or the scale for left and right panel is not the same. Neither legend nor methods describe how normalization was performed.*

Thank you for pointing this out, the figure has been corrected. We have updated the Materials and Methods (line 365) and have added codes and pipelines to GitHub to explain the normalisation procedure in more detail (https://github.com/Zhenhuiz/H1restricts-euchromatin-associated-methylation-pathways-from-heterochromaticencroachment).